

Structure-Based Approach for the Study of Estrogen Receptor Binding Affinity and Subtype Selectivity

Lívia B. Salum, Igor Polikarpov, and Adriano D. Andricopulo*

Laboratório de Química Medicinal e Computacional, Centro de Biotecnologia Molecular Estrutural,
Instituto de Física de São Carlos, Universidade de São Paulo, Av Trabalhador São-Carlense 400,
13560-970 São Carlos-SP, Brazil

Received June 27, 2008

Estrogens exert important physiological effects through the modulation of two human estrogen receptor (hER) subtypes, alpha (hER α) and beta (hER β). Because the levels and relative proportion of hER α and hER β differ significantly in different target cells, selective hER ligands could target specific tissues or pathways regulated by one receptor subtype without affecting the other. To understand the structural and chemical basis by which small molecule modulators are able to discriminate between the two subtypes, we have applied three-dimensional target-based approaches employing a series of potent hER-ligands. Comparative molecular field analysis (CoMFA) studies were applied to a data set of 81 hER modulators, for which binding affinity values were collected for both hER α and hER β . Significant statistical coefficients were obtained (hER α , $q^2 = 0.76$; hER β , $q^2 = 0.70$), indicating the internal consistency of the models. The generated models were validated using external test sets, and the predicted values were in good agreement with the experimental results. Five hER crystal structures were used in GRID/PCA investigations to generate molecular interaction fields (MIF) maps. hER α and hER β were separated using one factor. The resulting 3D information was integrated with the aim of revealing the most relevant structural features involved in hER subtype selectivity. The final QSAR and GRID/PCA models and the information gathered from 3D contour maps should be useful for the design of novel hER modulators with improved selectivity.

INTRODUCTION

Estrogens play a critical role in the development and metabolic homeostasis of various target tissues, including the reproductive tract, breast, nervous, and the cardiovascular and immune systems.^{1–3} Their physiological effects are mediated by two human estrogen receptor (hER) subtypes, alpha (hER α)⁴ and beta (hER β),⁵ that function as ligand-activated transcriptional regulators.^{6–8} The deficiency of estrogens is related to a range of symptoms experienced by menopausal women, including hot flashes, reduced bone density and mood swings. Steroids, commonly employed in current clinical practice for hormone replacement therapy (HRT), provide benefits by reducing menopausal symptoms and osteoporosis. However, the benefits of steroids are generally limited by severe side effects arising from disorders in endometrial function, comprising bleeding problems, endometrial proliferation, and even malignancy, as well as for the increased risk of breast cancer and fatal stroke during prolonged therapy.^{9–19}

Because of these important concerns, the interest in the development of tissue-selective modulators capable of retaining the beneficial effects of estrogens, while avoiding most of their undesired adverse effects, has been increasing in recent years.^{20–23} The nuclear receptors hER α and hER β show distinct pharmacological profiles, tissue distribution, and specific biological functions.^{5,20–26} The role of hER α in reproductive tissues and its impact on breast cancer

etiology and progression is well established.^{8,21,27} At the same time, it has been shown that hER β works as the counter partner of hER α in some tissues and is also associated with a favorable prognosis when expressed in breast cancer tissues.^{28,29} Furthermore, hER β is not the dominant hER expressed in the uterus.^{30–32} Epidemiological studies have indicated some positive effects of isoflavones (mainly, genistein and daidzein) on menopausal disorders, reducing the rates of breast and endometrial complications. These effects are caused by the selective binding to hER β and the recruitment of coregulator proteins that trigger hER β -mediated transcriptional pathways.^{31,33,34} These evidences make hER β an attractive drug target for the development of selective agonists.^{28,35}

The ligand-binding domains of the two subtypes share an overall 58% identity, while the ligand-binding cavities are almost identical, differing by only two amino acid residues of remarkably conservative characteristics (Leu384 and Met421 in hER α are replaced by Met336 and Ile373 in hER β , respectively). Thus, it is not surprising that 17 β -estradiol displays a similar affinity for both receptors.^{5,24,36,38,39} Nevertheless, a number of subtype-selective modulators with drug-like properties have been reported, suggesting new opportunities for drug design.^{26,30,32,36,39–42}

Structure-based approaches have become vital components of modern drug design.^{43,44} Quantitative structure–activity relationships (QSAR) have been successfully used as valuable tools to assist the design of small-molecule inhibitors or receptor ligands having promise of utility in clinical medicine.^{45–47} To better understand the chemical

* To whom correspondence should be addressed. E-mail: aandrico@ifsc.usp.br. Tel: + 55 16 3373-8095. Fax: + 55 16 3373-9881.

Table 1. Chemical Structures and Corresponding IC₅₀ Values (nM) for a Series of Human Estrogen Receptor Modulators

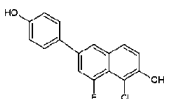
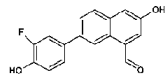
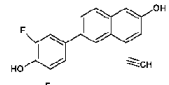
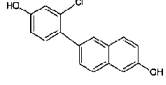
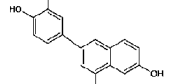
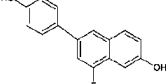
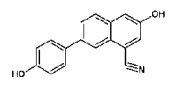
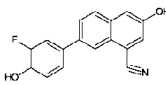
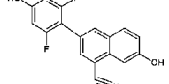
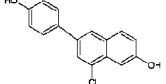
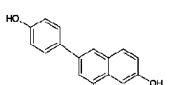
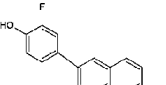
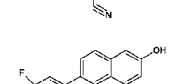
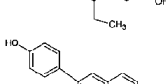
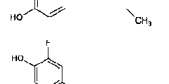
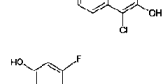
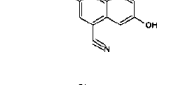
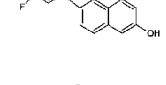
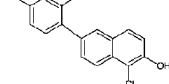
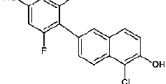
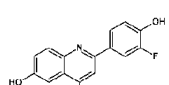
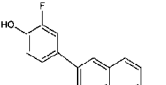
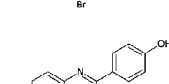
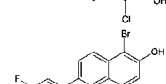
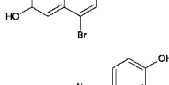
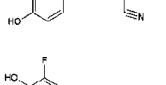
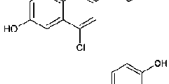
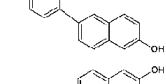
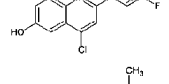
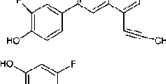
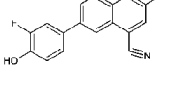
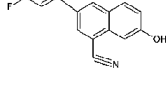
Compound	Structure	β IC ₅₀	α IC ₅₀	Compound	Structure	β IC ₅₀	α IC ₅₀
<i>Training set</i>							
1		1.1	40	2		1.1	73
3		1.2	73	4		1.4	10
5		1.5	21	6		1.6	22
7		2.0	84	8		2.1	96
9		2.2	45	10		2.3	30
11		2.3	105	12		2.4	235
13		2.5	113	14		2.5	91
15		2.7	210	16		2.8	27
17		3.3	36	18		3.4	35
19		3.4	283	20		4.0	143
21		4.3	212	22		4.5	116
23		4.6	213	24		5	92
25		5.3	246	26		5.5	180
27		6.0	406	28		6.9	186
29		7.0	77	30		7.3	527
31		8.4	92	32		8.5	118

Table 1. Continued

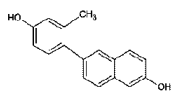
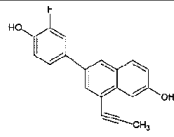
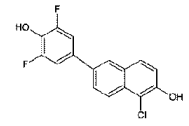
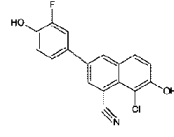
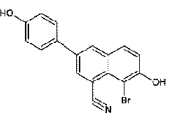
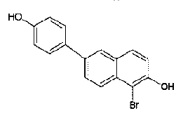
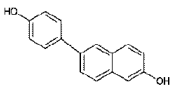
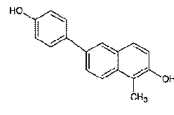
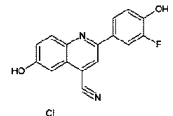
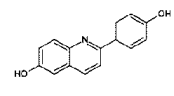
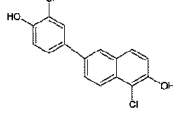
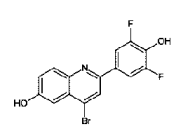
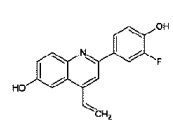
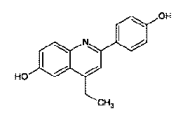
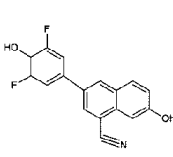
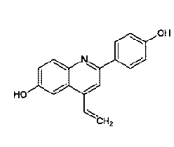
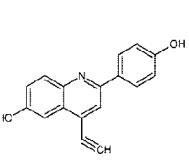
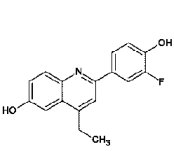
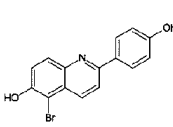
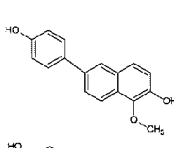
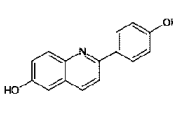
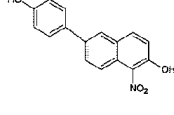
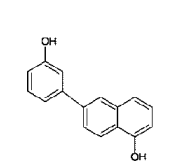
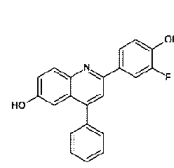
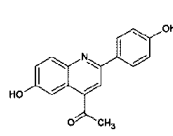
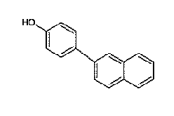
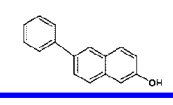
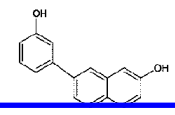
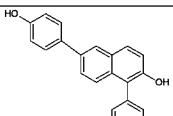
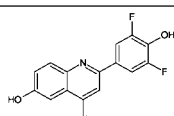
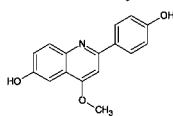
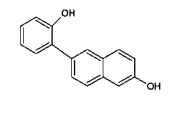
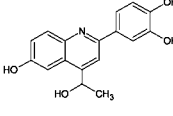
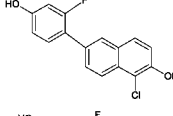
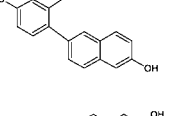
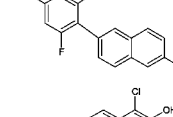
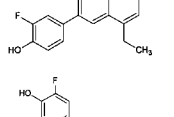
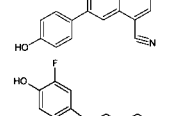
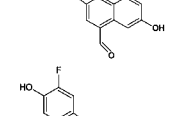
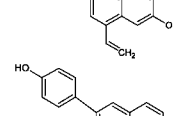
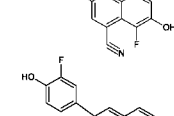
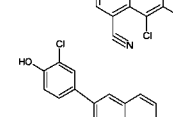
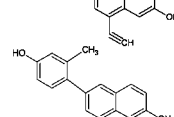
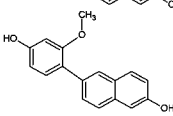
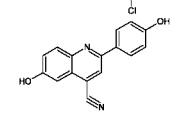
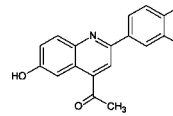
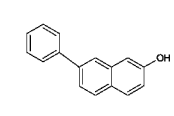
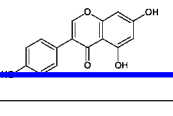
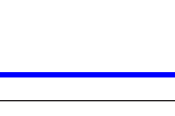
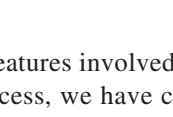
Compound	Structure	βIC_{50}	αIC_{50}	Compound	Structure	βIC_{50}	αIC_{50}
33		10	40	34		10	343
35		10.6	519	36		11	299
37		12	131	38		13	266
39		16.3	211	40		17	282
41		23	1047	42		30	632
43		32	356	44		36	783
45		44	385	46		52	634
47		58	548	48		60	504
49		75	1500	50		79	1750
51		88	1140	52		114	884
53		171	1775	54		199	709
55		205	1452	56		211	1815
57		221	3138	58		245	638
59		374	1345	60		566	2642

Table 1. Continued

Compound	Structure	βIC_{50}	αIC_{50}	Compound	Structure	βIC_{50}	αIC_{50}
61		748	1231	62		750	4820
63		1190	6630	64		2000	5000
65		5000	5000	<i>Test set</i>			
66		1.2	58	67		2	24
68		2.3	10,3	69		2.5	113
70		3	98	71		3.4	231
72		4.4	254	73		5.6	312
74		6	109	75		6.3	247
76		11	107	77		13	40
78		27	174	79		28	455
80		93	3370	81		527	3405
gen		9.7	395				

and structural features involved in the selective molecular recognition process, we have collected values of binding affinity for a series of hER α and hER β modulators,^{48,49} and used the data to create 3D QSAR CoMFA models that demonstrate substantial predictive capability. In addition, we have applied the GRID/PCA method for the characterization of five hER crystal structures, highlighting 3D regions that suggest potential sites for obtaining selectivity. The identification of the key structural and chemical features associated with affinity and selectivity should be valuable tools for the design of promising candidates for clinical development.

COMPUTATIONAL METHODS

Data Sets. The data set used for QSAR analyses contains 81 hER modulators that were collected from the literature.^{48,49} The structures and corresponding binding affinity data for both hER α and hER β are presented in Table 1.

Computational Approach. The QSAR and PCA modeling analyses, calculations, and visualizations for CoMFA and GRID were performed using the SYBYL 8.0 package (Tripos Inc., St. Louis, MO) and GRID 22 program (Molecular Discovery Ltd., Perugia, Italy), respectively, running on Red Hat Enterprise Linux workstations. The 3D structures of the small molecule modulators were

constructed using standard geometric parameters of the molecular modeling software package SYBYL 8.0. Each single optimized conformation of each molecule in the data set was energetically minimized employing the AM1 quantum mechanical method as implemented in MOPAC 6.0.

Alignment Rules. A docking protocol, as implemented in GOLD 2.1 (Cambridge Crystallographic Data Centre, Cambridge, U.K.), a genetic algorithm-based software, was employed to search the possible binding conformations of ligands into the ER ligand-binding sites. The X-ray crystallographic data (ER in complex with genistein) used in docking simulations were retrieved from the Protein Data Bank (PDB codes 1QKM for hER β and 1X7R for hER α). For the calculations, genistein and water molecules were removed, and hydrogen atoms were added in standard geometry. The ligand-binding sites were centered on the C7 atom of genistein, and a radius sphere of 10 Å was considered during the docking procedures. The energy-minimized structures of the ligands were used in the docking protocol, which was repeated 10 times for each molecule because of the stochastic nature of the search algorithm. Default parameters and the GOLDScore function were employed in all runs, and only the best ranked conformation of each ligand was considered for the 3D QSAR studies. The 3D conformation models were used for the structural alignment of the database ligands. The aligned molecules were then exported to SYBYL and employed in the QSAR studies.

3D QSAR CoMFA Analyses. The 3D QSAR studies were performed as previously described.^{45,50–54} The steric and electrostatic properties were calculated according to Lennard-Jones and Coulomb potentials, respectively. The aligned training set molecules were placed in a 3D grid box, and the corresponding CoMFA steric and electrostatic fields were generated at each grid point with Tripos force field using a sp³ carbon atom probe carrying a charge of +1 and a van der Waals radius of 1.52 Å. The CoMFA grid spacing of 1.0 Å in the *x*, *y*, and *z* directions, and the grid region were generated by the CoMFA routine to encompass all molecules with an extension of 2.0 Å in each direction. The CoMFA region focusing method was applied to increase the resolution of the CoMFA models. The default value of 30 kcal mol^{–1} was set as the maximum steric and electrostatic energy cutoff. All CoMFA models were investigated using the full cross-validated *r*² (*q*²) partial least-squares (PLS) leave-one-out (LOO) method. Leave-many-out (LMO) cross-validation with 5 and 10 randomly selected groups were used as a more rigorous test to assess model stability and statistical significance. Each random cross-validation run was repeated 25 times to obtain mean values for *q*² and the corresponding SDEP. Progressive scrambling method was applied to determine the sensitivity of the QSAR models to chance correlations. The CoMFA contour maps were generated by interpolation of the pairwise products between the PLS coefficients and standard deviations of the corresponding descriptors values. External model validation was performed with a test set of compounds, which were not considered for QSAR model generation. After generation of the PLS training set models, the dependent variables (pIC₅₀) were predicted for the test set compounds, allowing predictive-*r*² values to be determined for the individual 3D QSAR models.

Table 2. Human Estrogen Receptor Structures Used in the 3D Studies

structure (PDB code)	subtype	ligand
1X7R	hER α	genistein
1QKM	hER β	genistein
1X7E	hER α	WAY-244
1X78	hER β	WAY-244
1X7B	hER β	ERB-041

Estrogen Receptor 3D-Structure Studies. The coordinates of the five hERs X-ray crystal structures shown in Table 2 were retrieved from the PDB (PDB codes 1X7R, 1QKM, 1X7E, 1X78, and 1X7B) and superposed on one another using the C α atoms. Both ligands and water molecules were removed, and hydrogen atoms were added by the program GRIN. Potassium counterions were added using MINIM and FILMAP to eliminate large electrostatic differences between the receptor structures. A GRID box was chosen to fully enclose all the important positions around the ligand-binding site, resulting in a 16 × 12 × 15 Å cage. The GRID spacing was set to 0.5 Å in the *x*, *y*, and *z* directions. The multivariate characterization of the ligand-binding site by the nonbonded interaction energies between the hER structures and the DRY and OH2 chemical groups was investigated with the GRID force field. The MOVE option in the GRID program was used to allow lone pairs, tautomeric hydrogen atoms, and the torsion angle of groups such as sp³ hydroxyl or sp² amine to alter, in response to the probes. Statistical evaluation of the obtained fields was performed using the principal component analysis (PCA), as implemented in SYBYL 8.0, with pretreated and scaled variables to take into account the very different interaction energies obtained with the two different probes. Only negative interaction values were considered.

RESULTS AND DISCUSSION

Data Set Characterization. 3D QSAR CoMFA models were derived for a series of 81 estrogen receptor modulators to which binding affinity measurements for both hER α and hER β were collected (Table 1). The chemical diversity of the data set is represented by 6-phenylnaphthalenes and 2-phenylquinolines, which were developed to mimic the genistein framework, a modest hER β -selective modulator. The values of binding affinity (as measured by IC₅₀ values) vary from 1.1 to 5000 nM to hER β (a factor of 4500) and from 10 to 6630 nM to hER α (a factor of 663) and are acceptably distributed across the range of values. This data set was selected because the compounds provided an appropriate structural diversity for QSAR modeling and the associated biological data were of high quality.

The generation of reliable statistical models is dependent on the creation of appropriate training and test sets. From the original data set of 81 modulators, 65 compounds were selected as members of the training set for model construction (1–65, Table 1) and the remaining 16 compounds (66–81, Table 1) were defined as members of the test set for external model validation. Hierarchical cluster analyses performed with Tsar 3D (Accelrys, San Diego, CA) was used as previously described to guide an appropriate compound selection.^{51,54} Training and test sets were selected in such a way that structurally diverse molecules possessing activities

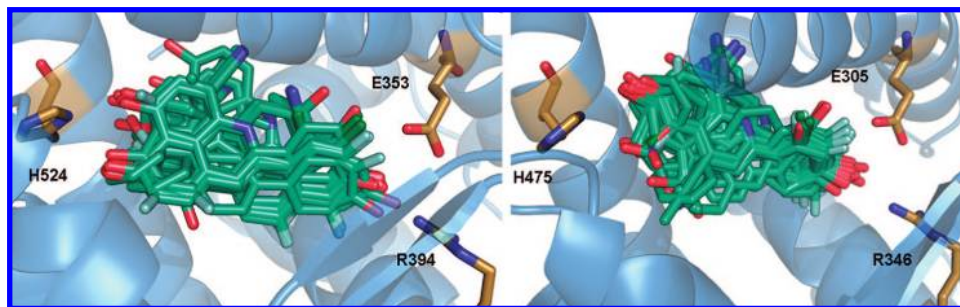


Figure 1. Alignment of the data set molecules for conformations generated by GOLD 2.1. The PDB codes are 1X7R for the hER α alignment (left) and 1QKM for hER β (right).

of a wide range were included in both sets. Thus, the data set is appropriate for the purpose of QSAR model development. The same training and test sets were employed for all 3D QSAR analyses. The IC₅₀ values were converted into the corresponding pIC₅₀ (−log IC₅₀) values and used as dependent variables in the investigations. The PLS method was used for all 3D QSAR analyses. The predictive ability of the models was assessed by their q^2 values and by test set predictions.

Structural Alignment. The best ranked conformation obtained from the docking procedures for each modulator was used in the QSAR studies. Following the alignment of the data set compounds, each conformation was individually inspected, and no particular problem was found. As can be seen in Figure 1, the 3D alignments obtained with the same data set of ligands for the two hER subtypes are significantly different from each other, revealing important ligand–receptor selectivity. These results are very interesting and indicate a great potential for selective-modulator design, even in this case, where the main amino acid residues involved in hydrogen bonding interactions are notably conserved in both hER cavities.^{8,21,36,45,54–56} For example, His524, Arg394, and Glu353 in hER α have their respective partners His475, Arg346, and Glu305 in hER β . However, slight modifications (Leu384/Met336 and Met421/Ile373) along with the protein subtype conformational changes caused by ligand-binding may influence affinity and determine key 3D structural features for selectivity.

CoMFA Models. The CoMFA approach is based on the assumption that changes in binding affinities are related to changes in molecular properties represented by 3D steric and electrostatic fields. The alignment rule is a crucial component in 3D QSAR studies, affecting the calculations of the fields and the results of the statistical analyses. Because we have used the same set of ligands for the molecular alignment in the hER α and hER β cavities, the significant conformational changes observed in the two structural alignments are caused by variations in the hER cavities; therefore, steric and electrostatic fields play important roles in the control of binding-affinity and hER subtype selectivity.

The 3D alignments shown in Figure 1 were submitted to the CoMFA analyses, and the models were optimized through the CoMFA region focusing method.^{51,52} The region focusing was weighted by StDev*Coefficient values ranging from 0.3 to 1.5 and grid spacing ranging from 0.5 to 2.0. This strategy not only increased q^2 values during the process of model generation but also resulted in the refinement of 3D contour maps. The best statistical results are presented in Table 3. As can be seen, the data revealed significant statistical

Table 3. COMFA Results^a

subtype	q^2	N	r^2	SEE	F	fraction	
						S	E
hER α	0.76	8	0.94	0.19	118.9	0.49	0.51
hER β	0.73	8	0.96	0.17	184.9	0.41	0.59

^a q^2 , leave-one-out (LOO) cross-validated correlation coefficient; N, optimum number of components; r^2 , non-cross-validated correlation coefficient; SEE, standard error of estimate; F , F -test value; S , steric field; E , electrostatic field.

correlation coefficients for the generated QSAR models. A cross-validated correlation coefficient q^2 of 0.76 and a conventional non cross-validated correlation coefficient r^2 of 0.94 with a standard error of estimate (SEE) of 0.19 were obtained for the hER α CoMFA model, while a q^2 of 0.73 and an r^2 of 0.96 (SEE = 0.17) were obtained for the hER β model. In both cases, the results confirm the stability and reliability of the 3D QSAR models, considering that the statistical values obtained for the LMO analyses are comparable to those of the LOO analysis. Progressive scrambling of the data set was also carried out to check for possible chance correlations and to test the stability of the models. The results further confirmed consistency of the models as defined by the critical slope, and optimum statistics for cSDEP and Q²*² obtained at the end of different runs.

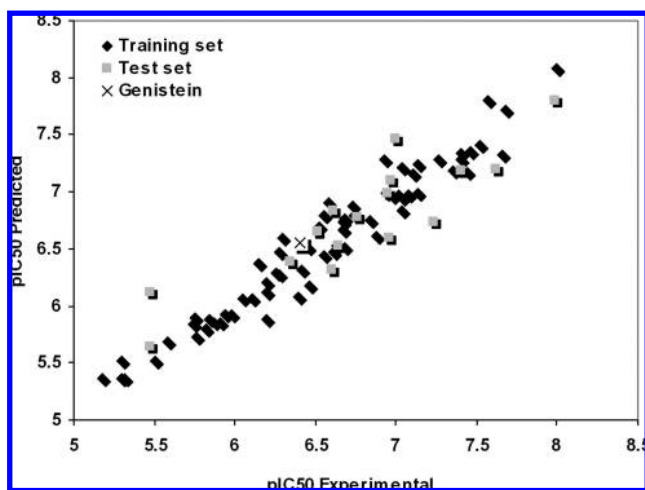
The predictive ability of the internally consistent CoMFA models generated employing the 65 training set molecules (compounds 1–65, Table 1) was assessed by predicting biological activities of an external test set (compounds 66–81, Table 1). The external validation is the most valuable method to evaluate the predictive ability of the models because the test set compounds were completely excluded during the generation of the models. Prior to prediction, the test set compounds were processed identically to the training set compounds, as previously described. The results are listed in Tables 4 and 5, and the graphic results simultaneously displayed in Figures 2 and 3. The predicted values fall close to the experimental pIC₅₀ values, not deviating by more than 0.5 log units, except for compound 66, for which the predicted value (for hER α) is more substantially in error (0.65 units). Interestingly, no outliers were detected in this series of hER modulators. Predictive r^2 values of 0.80 and 0.88 were obtained for hER α and hER β CoMFA models, respectively. The good agreement between actual and predicted pIC₅₀ values for the test set compounds in both 3D QSAR models suggests that the constructed models are reliable and can be used for the design of modulators with improved binding affinity and selectivity.

Table 4. Experimental and Predicted Activities for hER α (α pIC₅₀) with Residual Values for the Test Set Compounds

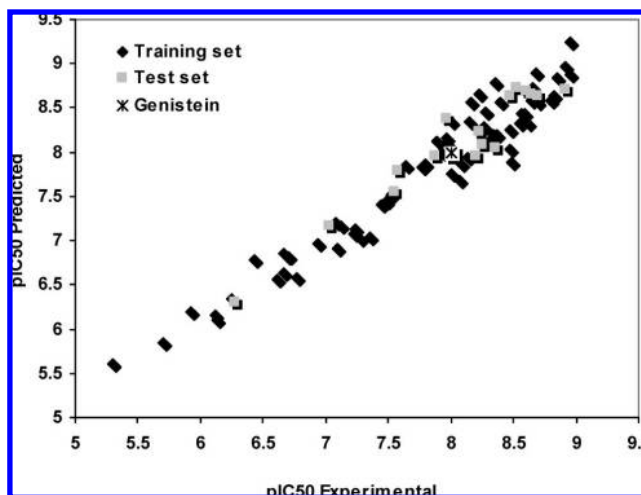
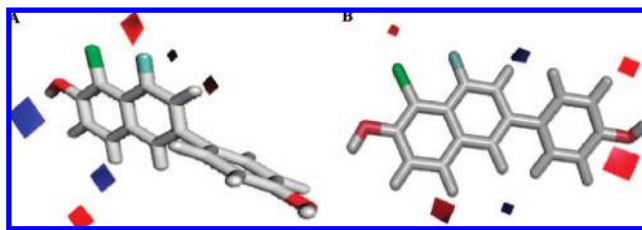
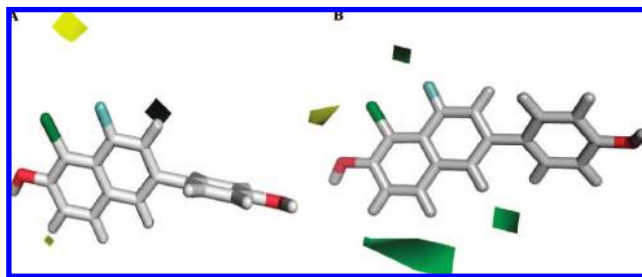
test set compound	pIC ₅₀ Experimental	pIC ₅₀ predicted	residuals ^a
66	5.47	6.12	-0.65
67	5.47	5.65	-0.18
68	6.34	6.39	-0.05
69	6.76	6.78	-0.02
70	7.40	7.19	0.21
71	6.97	7.10	-0.13
72	6.61	6.84	-0.23
73	6.96	6.60	0.36
74	6.51	6.65	-0.14
75	6.60	6.31	0.29
76	6.64	6.52	0.12
77	7.00	7.46	-0.46
78	6.95	6.99	-0.04
79	7.99	7.80	0.19
80	7.62	7.20	0.42
81	7.23	6.73	0.50
genistein	6.40	6.55	-0.15

^a The difference between experimental and predicted values.**Table 5.** Experimental and Predicted Activities for hER β (β pIC₅₀) with Residual Values for the Test Set Compounds

test set compound	pIC ₅₀ experimental	pIC ₅₀ predicted	residuals ^a
66	6.28	6.32	-0.04
67	7.03	7.43	-0.40
68	7.55	7.18	0.37
69	7.57	7.86	-0.29
70	7.87	8.03	-0.16
71	7.96	8.25	-0.29
72	8.20	8.10	0.10
73	8.22	8.23	-0.01
74	8.25	8.16	0.09
75	8.36	8.15	0.21
76	8.47	8.94	-0.47
77	8.52	8.63	-0.11
78	8.60	8.81	-0.21
79	8.64	8.60	0.04
80	8.70	8.95	-0.25
81	8.92	8.64	0.28
genistein	8.01	7.77	0.24

^a The difference between experimental and predicted values.**Figure 2.** Plot of predicted vs corresponding experimental values for training and test sets for the hER α model.

The understanding of protein–ligand interactions is essential for the design of selective compounds with improved affinity. In addition to prediction of the property value of

**Figure 3.** Plot of predicted vs corresponding experimental values for training and test sets for the hER β model.**Figure 4.** CoMFA electrostatic contour maps (SD \times coefficient): (A) model for hER α and (B) model for hER β . Higher values of binding affinity are correlated with more positive charge near blue and more negative charge near red. The derivative with the highest β -affinity, **1**, is displayed in the background for reference.**Figure 5.** CoMFA steric contour maps (SD \times coefficient): (A) model for hER α and (B) model for hER β . Greater values of the affinity are correlated with more bulk near green and less bulk near yellow. The derivative with the highest β -affinity, **1**, is displayed in the background for reference.

interest for untested molecules, 3D QSAR models should also provide insights into molecular properties directly related to biological activity. One prominent feature of the 3D QSAR method employed in this study is the easy visualization of regions in space responsible for increases or decreases in the values of a particular type of dependent variable (e.g., pIC₅₀).

CoMFA steric field descriptor for hER α model explains 49% of the total variance, while the electrostatic descriptor accounts for 51%. For hER β , steric and electrostatic fields explain 41% and 59%, respectively. These results indicate that the electrostatic fields play a more important role in the hER β CoMFA model than it does in the hER α model. These observations are in agreement with previous studies that indicate that the substitution of methionine by isoleucine at

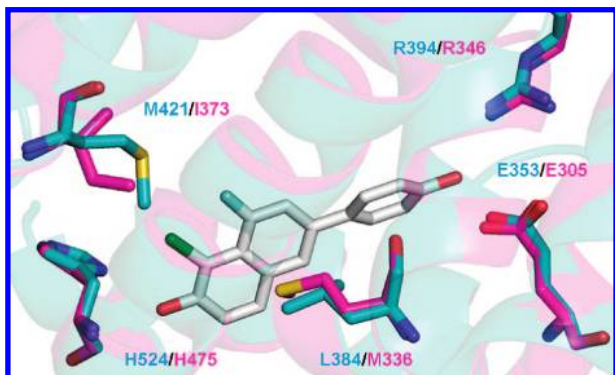


Figure 6. Representation of the binding mode of the highest β -affinity modulator (gray, modulator **1**) into the crystal structures of hER subtypes. The substituted residues in hER α (cyan) and hER β (pink) surround positions 1 and 8 in the naphthalene ring.

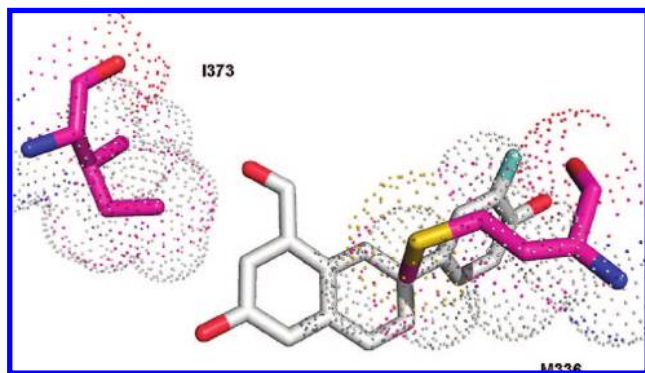


Figure 7. Representation of the potential interaction of modulator **2** (gray) with Met336 in the hER β ligand-binding site.

position 373 results in the accommodation of more-polar substituents in hER β .^{38,57}

The CoMFA electrostatic contour maps for hER α and hER β are shown in Figure 4 as PLS StDev*Coefficient plots, along with the highest affinity hER β modulator (compound **1**). The corresponding steric fields are depicted in Figure 5. A comparison between the hER α and hER β contour maps reveals some important similarities, with the substituents at positions 2, 4, 5, and 7 in the naphthalene ring strongly associated to binding affinity for both subtypes. It is likely that structural modifications at these positions would increase affinity without affecting selectivity. As shown in the electrostatic maps (Figure 4), the presence of electronegative groups at positions 1 and 8 (chlorine and fluorine substituents of modulator **1**) is related to increased binding-affinity for the two ER subtypes. However, as shown in the steric maps (Figure 5), the introduction of bulkier substituents with this physicochemical characteristic is only possible in hER β . Additionally, electronegative substituents at 3'-position of the phenyl ring are considered favorable contributions to hER β affinity in comparison to hER α (Figure 4). The identification of these important structural features should be useful for the design of novel ER ligands with improved subtype selectivity.

The 3D QSAR models generated in this study are compatible with the 3D protein environment in the ER binding site as shown in Figure 6. As can be seen, the positions 1 and 8 are surrounded by the two amino acid residues that differ in the ligand-binding pocket of hER α and hER β . A more bulky electronegative substituent at

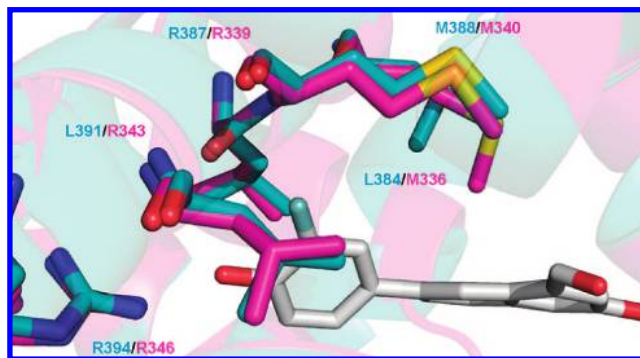


Figure 8. Representation of the binding mode of the modulator **2** (gray) into the crystal structures of hER subtypes, hER α (cyan) and hER β (pink). The 3'-fluoro group is surrounded by the branched side chain of Leu384 (hER α) and the linear chain of Met336 (hER β).

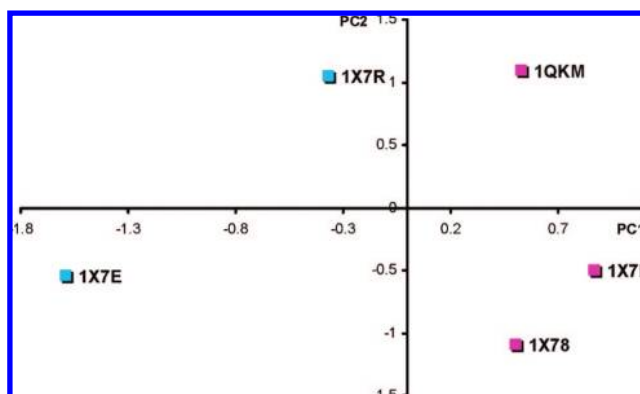


Figure 9. PC1 versus PC2 score plot for the GRID probes within the ER ligand-binding site. PC1 can be used to discriminate between hER α (cyan) and hER β (pink), whereas PC2 discriminates conformational changes related to different ligands.

position 1 of the naphthalene ring would sterically clash with the Met421 side chain in hER α (but not Ile373 in hER β), resulting in unfavorable intermolecular interactions.^{39,58,59}

Previous studies have demonstrated the important role of residue Met336 in determining hER β -ligand selectivity.^{38,39} In this respect, the sulfur atom of Met336, having high electronic density, would approach the side of the electronic deficiency of the substituent at position 1 on the naphthalene scaffold, and therefore, energetically favorable interactions could take place between orbitals of the sulfur atom and those of the ligand. Similar favorable interactions would not occur between the Leu384 residue in hER α and the group at position 1 of the naphthalene ring, therefore, explaining the hER β -selective characteristics of modulators **2**, **3**, **15**, **27**, and **30**. Modulator **2**, for example, possesses a carbonyl substituent at position 1 of the naphthalene ring, which interacts with Met336, as depicted in Figure 7. The aforementioned two mechanisms can be combined as a complementary approach for the assessment of hER subtype selectivity.

Leu384 (hER α)/Met336 (hER β) substitution can also explain the importance of electronegative substituents at the 3'-position of the phenyl ring for β -selectivity. The linear side chain of Met336 in hER β accommodates the electronegative 3'-substituent of the modulator, which can favorably interact with positively charged groups of the Arg346 side chain and the amide hydrogen of Leu343. However, the more hydrophobic and branched side chain of Leu384 in hER α

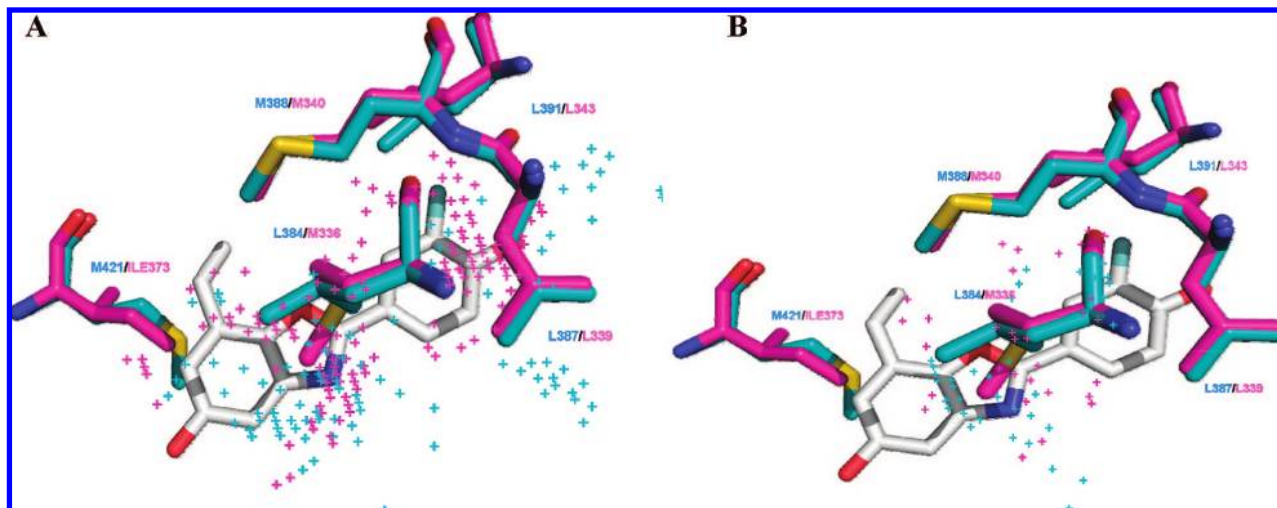


Figure 10. Isocontour maps from high PC1 loadings: (A) OH2 probe and (B) DRY probe. Regions involved in hER α discrimination are displayed in cyan and hER β in pink. Some residues are shown for hER α (cyan) and hER β (pink). The ER041 β -selective modulator is displayed as reference.

penalizes the presence of the electronegative substituent at this position, as depicted in Figure 8 for modulator **2**. The understanding of these molecular connections is especially attractive for further SAR studies with the aim of developing new molecules with interesting profile. The 3D CoMFA contour maps are useful tools for the design of novel selective modulators with improved affinity.

GRID/PCA Models. The availability of 3D structures of the target proteins allows the search for subtype-selective ligands by looking at differences in sequence or structure of the different subtypes, which could be exploited for selective target-ligand interactions. The integrated information obtained from different 3D processes is a valuable strategy in drug design. In this context, we have collected five hER structures (Table 2) and studied the structural differences between hER α and hER β . Because of the high flexibility of the hER ligand-binding cavities, which allows the accommodation of a variety of structurally diverse small molecule ligands,^{1,2,7,8} we have selected structures of the hER subtypes in complex with the same ligands. Additionally, we have used a structure of hER β in complex with a known β -selective ligand (ERB041).

The GRID method was used to quantify the interactions between the GRID probes OH2 and DRY, which represent hydrophilic and hydrophobic intermolecular interactions, respectively, and the molecular environment of hER (protein atoms included in a GRID cage), comprising the ligand-binding cavities. Principal components analysis (PCA), a well-known multivariate analysis technique, was used to highlight the most relevant differences in the target proteins.^{60–64} The evaluation of the differences as expressed by interaction energies with the hydrophilic and hydrophobic probes resulted in two PCs explaining 67% of the overall variance. The score plot for this model is shown in Figure 9.

As can be seen in Figure 9, the first PC, which accounts for 41% of the total variance, distinguishes between the two receptor subtypes, clustering the objects into two groups: hER α structures, positioned in PC1 negative values, and hER β structures, located in positive values. This ability of PC1 to discern between the probe–receptor interactions suggest that structural differences can be explored in the design of selective ligands. Variables with high PC1 loadings

delimit regions of the ligand-binding site where both hydrophilic and hydrophobic probes show an extremely different behavior in their interaction with the two receptor subtypes. Because only favorable interactions were considered, these regions revealed important positions for the incorporation of new hydrophobic or hydrophilic groups, as chemical determinants for selective binding to α and β subtypes. To better visualize this principle, the high PC1 loadings for each probe were translated into pseudocontour plots. The 3D pseudocontour maps showing PC1 loadings higher than 0.90 for the OH2 probe, representing the relevant regions highlighted by the statistical model, are shown in Figure 10A, while the corresponding maps for the DRY probe are displayed in Figure 10B.

As can be seen in Figure 10, the regions surrounded by the two different amino acid residues in the hER subtypes (hER β Met336/Leu384 hER α ; hER β Ile373/Met421 hER α) are important to discriminate between the two. As it concerns the design of selective ligands, bulky groups capable of establishing electrostatic interactions with the sulfur atom of Leu336 are associated with hER β selectivity, which is in agreement with the QSAR 3D CoMFA results.^{39,58,59} Furthermore, the regions of hER β enclosing the Leu343, Met340, and Leu339 side chains (Leu391, Met388, and Leu387, respectively, in hER α) represent positions, where the probes could establish β -selective electrostatic interactions. The mechanisms underlying these observations are unclear and need to be investigated in more detail, considering that the amino acid residues are conserved between the two hER (α and β) subtypes.^{30,58,65} However, as previously discussed (Figure 8), favorable interactions of a 3'-phenyl electronegative group with the surrounding amino acid residues are possibly prevented because of the character of Leu384 in hER α . Then, this region represents a position where a hydrophilic group could be incorporated in novel β -selective ligands. On the other hand, PC2, which explains 26% of the total variance, is approximately able to discern conformational changes that are provoked by different ligands (genistein and WAY-244), being related with non-selective ligand-target interactions.

The several similarities between the GRID/PCA pseudocontour plots and QSAR 3D CoMFA contour maps suggests

that, despite slight variation between the two binding cavities of the hER subtypes, it is possible to explore structural and conformational differences for the design of potent hER modulators with improved subtype selectivity.

ACKNOWLEDGMENT

We gratefully acknowledge financial support from the Brazilian grant agencies FINEP (Research and Projects Financing) and FAPESP (The State of São Paulo Research Foundation). We also thank the IIPF (International Institute of Pharmaceutical Research) from the Pharmaceutical Group EMS Sigma Pharma for a long and stimulating scientific collaboration.

REFERENCES AND NOTES

- Nilsson, S.; Gustafsson, J.-Å. Biological Role of Estrogen and Estrogen Receptors. *Crit. Rev. Biochem. Mol. Biol.* **2002**, *37*, 1–28.
- Osborne, C. K.; Schiff, R. Estrogen-Receptor Biology: Continuing Progress and Therapeutic Implications. *J. Clin. Oncol.* **2005**, *23*, 1616–1622.
- Gruber, C. J.; Tschugguel, W.; Schneeberger, C.; Huber, J. C. Production and Actions of Estrogens. *N. Engl. J. Med.* **2002**, *346*, 340–352.
- Green, S.; Walter, P.; Kumar, V.; Krust, A.; Bornert, J. M.; Argos, P.; Chambon, P. Human Oestrogen Receptor cDNA: Sequence, Expression and Homology to v-erb-A. *Nature* **1986**, *320*, 134–139.
- Mosselman, S.; Polman, J.; Dijkema, R. ER β : Identification and Characterization of a Novel Human Estrogen Receptor. *FEBS Lett.* **1996**, *392*, 49–53.
- Gustafsson, J.-Å. What Pharmacologists Can Learn from Recent Advances in Oestrogen Signaling. *Trends Pharmacol. Sci.* **2003**, *24*, 479–485.
- Gronemeyer, H.; Gustafsson, J.-Å.; Laudet, V. Principles for Modulation of the Nuclear Receptor Superfamily. *Nat. Rev. Drug Discovery* **2004**, *3*, 950–964.
- Jordan, V. C. Antiestrogens and Selective Estrogen Receptor Modulators as Multifunctional Medicines. 1. Receptor Interactions. *J. Med. Chem.* **2003**, *46*, 883–908.
- Khan, S. A.; Pace, J. E.; Cox, M. L.; Gau, D. W.; Cox, S. A.; Hodgkinson, H. M. Climacteric Symptoms in Healthy Middle-aged Women. *Br. J. Clin. Pract.* **1994**, *48*, 240–242.
- Sherwin, B. B. Hormones, Mood, and Cognitive Functioning in Postmenopausal Women. *Obstet. Gynecol.* **1996**, *87*, S20–S26.
- Palacios, S. Current Perspectives on the Benefits of HRT in Menopausal Women. *Maturitas* **1999**, *33*, S1–S13.
- MacLennan, A.; Lester, S.; Moore, V. Oral Estrogen Replacement Therapy Versus Placebo for Hot Flashes: A Systematic Review. *Climacteric* **2001**, *4*, 58–74.
- Vestergaard, P.; Rejnmark, L.; Mosekilde, L. Fracture Reducing Potential of Hormone Replacement Therapy on a Population Level. *Maturitas* **2006**, *54*, 285–293.
- Kenemans, P.; van Unnik, G. A.; Mijatovic, V.; van der Mooren, M. J. Perspectives in Hormone Replacement Therapy. *Maturitas* **2001**, *38*, S41–S48.
- Barnabei, V. M.; Grady, D.; Stovall, D. W.; Cauley, J. A.; Lin, F.; Stuenkel, C. A.; Stefanick, M. L.; Pickar, J. H. Menopausal Symptoms in Older Women and the Effects of Treatment with Hormone Therapy. *J. Obstet. Gynecol.* **2002**, *100*, 1209–1218.
- Bhavnani, B. R.; Strickler, R. C. Menopausal Hormone Therapy. *J. Obstet. Gynaecol. Can.* **2005**, *27*, 137–162.
- Fernandez, E.; Gallus, S.; Bosetti, C.; Franceschi, S.; Negri, E.; La Vecchia, C. Hormone Replacement Therapy and Cancer Risk: A Systematic Analysis from a Network of Case-control Studies. *Int. J. Cancer* **2003**, *105*, 408–412.
- Gambacciani, M.; Monteleone, P.; Sacco, A.; Genazzani, A. R. Hormone Replacement Therapy and Endometrial, Ovarian and Colorectal Cancer. *Best Pract. Res. Clin. Endocrinol. Metab.* **2003**, *17*, 139–147.
- Yeh, I. T. Postmenopausal Hormone Replacement Therapy: Endometrial and Breast Effects. *Adv. Anat. Pathol.* **2007**, *14*, 17–24.
- Katzenellenbogen, B. S.; Choi, I.; Delage-Mouroux, R.; Ediger, T. R.; Martini, P. G.; Montano, M.; Sun, J.; Weis, K.; Katzenellenbogen, J. A. Molecular Mechanisms of Estrogen Action: Selective Ligands and Receptor Pharmacology. *J. Steroid Biochem. Mol. Biol.* **2000**, *74*, 279–285.
- Jordan, V. C. Antiestrogens and Selective Estrogen Receptor Modulators as Multifunctional Medicines. 2. Clinical Considerations and New Agents. *J. Med. Chem.* **2003**, *46*, 1081–1111.
- Katzenellenbogen, B. S.; Montano, M. M.; Ediger, T. R.; Sun, J.; Ekena, K.; Lazennec, G.; Martini, P. G.; McInerney, E. M.; Delage-Mouroux, R.; Weis, K.; Katzenellenbogen, J. A. Estrogen Receptors: Selective Ligands, Partners, and Distinctive Pharmacology. *Recent Prog. Horm. Res.* **2000**, *55*, 163–193.
- Veeneman, G. H. Non-steroidal Subtype Selective Estrogens. *Curr. Med. Chem.* **2005**, *12*, 1077–1136.
- Kuiper, G. G.; Carlsson, B.; Grandien, K.; Enmark, E.; Häggblad, J.; Nilsson, S.; Gustafsson, J. A. Comparison of the Ligand-Binding Specificity and Transcript Tissue Distribution of Estrogen Receptors Alpha and Beta. *Endocrinology* **1997**, *138*, 863–870.
- Couse, J. F.; Lindzey, J.; Grandien, K.; Gustafsson, J. A.; Korach, K. S. Tissue Distribution and Quantitative Analysis of Estrogen Receptor- α (ER α) and Estrogen Receptor- β (ER β) Messenger Ribonucleic Acid in the Wild-type and ER α -knockout Mouse. *Endocrinology* **1997**, *138*, 4613–4621.
- Barkhem, T.; Carlsson, B.; Nilsson, Y.; Enmark, E.; Gustafsson, J.; Nilsson, S. Differential Response of Estrogen Receptor α and Estrogen Receptor β to Partial Estrogen Agonists/antagonists. *Mol. Pharmacol.* **1998**, *54*, 105–112.
- Ariazi, E. A.; Ariazi, J. L.; Cordera, F.; Jordan, V. C. Estrogen Receptors as Therapeutic Targets in Breast Cancer. *Curr. Top. Med. Chem.* **2006**, *6*, 181–202.
- Saji, S.; Hirose, M.; Toi, M. Clinical Significance of Estrogen Receptor β in Breast Cancer. *Cancer Chemother. Pharmacol.* **2005**, *56*, 21–26.
- Shaaban, A. M.; O'Neill, P. A.; Davies, M. P.; Sibson, R.; West, C. R.; Smith, P. H.; Foster, C. S. Declining Estrogen Receptor- β Expression Defines Malignant Progression of Human Breast Neoplasia. *Am. J. Surg. Pathol.* **2003**, *27*, 1502–1512.
- Malamas, M. S.; Manas, E. S.; McDevitt, R. E.; Gunawan, I.; Xu, Z. B.; Collini, M. D.; Miller, C. P.; Dinh, T.; Henderson, R. A.; Keith, J. C. Jr.; Harris, H. A. Design and Synthesis of Aryl Diphenolic Azoles as Potent and Selective Estrogen Receptor- β Ligands. *J. Med. Chem.* **2004**, *47*, 5021–5040.
- Mäkelä, S.; Savolainen, H.; Aavik, E.; Myllärniemi, M.; Strauss, L.; Taskinen, E.; Gustafsson, J. A.; Häyry, P. Differentiation Between Vasculoprotective and Uterotrophic Effects of Ligands with Different Binding Affinities to Estrogen Receptors α and β . *Proc. Natl. Acad. Sci. U. S. A.* **1999**, *96*, 7077–7782.
- Harris, H. A.; Albert, L. M.; Leathurby, Y.; Malamas, M. S.; Mewshaw, R. E.; Miller, C. P.; Kharode, Y. P.; Marzolf, J.; Komm, B. S.; Winneker, R. C.; Frail, D. E.; Henderson, R. A.; Zhu, Y.; Keith, J. C., Jr. Evaluation of an Estrogen Receptor- β Agonist in Animal Models of Human Disease. *Endocrinology* **2003**, *144*, 4241–4249.
- McCarty, M. F. Isoflavones Made Simple—Genistein's Agonist Activity for the Beta-type Estrogen Receptor Mediates their Health Benefits. *Med. Hypotheses* **2006**, *66*, 1093–1114.
- Kuiper, G. G.; Lemmen, J. G.; Carlsson, B.; Corton, J. C.; Safe, S. H.; van der Saag, P. T.; van der Burg, B.; Gustafsson, J. A. Interaction of Estrogenic Chemicals and Phytoestrogens with Estrogen Receptor β . *Endocrinology* **1998**, *139*, 4252–4263.
- Nilsson, S.; Kuiper, G.; Gustafsson, J.-A. ER β : A Novel Estrogen Receptor Offers the Potential for New Drug Development. *Trends Endocrinol. Metab.* **1998**, *9*, 387–395.
- Miller, C. P.; Collini, M. D.; Harris, H. A. Constrained Phytoestrogens and Analogues as ER β Selective Ligands. *Bioorg. Med. Chem. Lett.* **2003**, *13*, 2399–2403.
- An, J.; Tzarakis-Foster, C.; Scharschmidt, T. C.; Lomri, N.; Leitman, D. C. Estrogen Receptor β -Selective Transcriptional Activity and Recruitment of Coregulators by Phytoestrogens. *J. Biol. Chem.* **2001**, *276*, 17808–17814.
- Pike, A. C.; Brzozowski, A. M.; Hubbard, R. E.; Bonn, T.; Thorsell, A. G.; Engström, O.; Ljunggren, J.; Gustafsson, J. A.; Carlquist, M. Structure of the Ligand-Binding Domain of Oestrogen Receptor Beta in the Presence of a Partial Agonist and a Full Antagonist. *EMBO J.* **1999**, *18*, 4608–4618.
- Sun, J.; Baudry, J.; Katzenellenbogen, J. A.; Katzenellenbogen, B. S. Molecular Basis for the Subtype Discrimination of the Estrogen Receptor- β -Selective Ligand, Diarylpropionitrile. *Mol. Endocrinol.* **2003**, *17*, 247–258.
- Güngör, T.; Chen, Y.; Golla, R.; Ma, Z.; Corte, J. R.; Northrop, J. P.; Bin, B.; Dickson, J. K.; Stouch, T.; Zhou, R.; Johnson, S. E.; Seethala, R.; Feyen, J. H. Synthesis and Characterization of 3-Arylquinazolinone and 3-Arylquinazolinethione Derivatives as Selective Estrogen Receptor Beta Modulators. *J. Med. Chem.* **2006**, *49*, 2440–2455.
- Richardson, T. I.; Dodge, J. A.; Wang, Y.; Durbin, J. D.; Krishnan, V.; Norman, B. H. Benzopyrans as Selective Estrogen Receptor β Agonists (SERBAs). Part 5: Combined A- and C-ring Structure-activity Relationship Studies. *Bioorg. Med. Chem. Lett.* **2007**, *17*, 5563–5566.
- Sprefico, M.; Boriani, E.; Benfenati, E.; Novic, M. Structural Features of Diverse Ligands Influencing Binding Affinities to Estrogen α and

- Estrogen β Receptors. Part II. Molecular Descriptors Calculated from Conformation of the Ligands in the Complex Resulting from Previous Docking Study. *Mol. Diversity* **2007**, *11*, 171–181.
- (43) Guido, R. V. C.; Oliva, G.; Andricopulo, A. D. Virtual Screening and Its Integration with Modern Drug Design Technologies. *Curr. Med. Chem.* **2008**, *15*, 37–46.
- (44) Andricopulo, A. D.; Montanari, C. A. Structure–Activity Relationships for the Design of Small-Molecule Inhibitors. *Mini-Rev. Med. Chem.* **2005**, *5*, 585–593.
- (45) Salum, L. B.; Polikarpov, I.; Andricopulo, A. D. Structural and Chemical Basis for Enhanced Affinity and Potency for a Large Series of Estrogen Receptor Ligands: 2D and 3D QSAR Studies. *J. Mol. Graph. Modell.* **2007**, *26*, 434–442.
- (46) Honório, K. M.; Garratt, R.; Andricopulo, A. D. Hologram Quantitative Structure Activity Relationships for a Series of Farnesoid X Receptor Activators. *Bioorg. Med. Chem. Lett.* **2005**, *15*, 3119–3125.
- (47) Moda, T. L.; Montanari, C. A.; Andricopulo, A. D. Hologram QSAR Model for the Prediction of Human Oral Bioavailability. *Bioorg. Med. Chem.* **2007**, *15*, 7738–7745.
- (48) Mewshaw, R. E.; Edsall, R. J., Jr.; Yang, C.; Manas, E. S.; Xu, Z. B.; Henderson, R. A.; Keith, J. C., Jr.; Harris, H. A. ER β Ligands. 3. Exploiting Two Binding Orientations of the 2-Phenyl-naphthalene Scaffold to Achieve ER β Selectivity. *J. Med. Chem.* **2005**, *48*, 3953–3979.
- (49) Vu, A. T.; Cohn, S. T.; Manas, E. S.; Harris, H. A.; Mewshaw, R. E. ER β Ligands. Part 4: Synthesis and Structure–Activity Relationships of a Series of 2-phenylquinoline Derivative. *Bioorg. Med. Chem. Lett.* **2005**, *15*, 4520–4525.
- (50) Guido, R. V. C.; Oliva, G.; Montanari, C. A.; Andricopulo, A. D. Structural Basis for Selective Inhibition of Trypanosomatid Glycer-aldehyde-3-Phosphate Dehydrogenase: Molecular Docking and 3D QSAR Studies. *J. Chem. Inf. Model.* **2008**, *48*, 918–929.
- (51) Castilho, M. S.; Postigo, M. P.; de Paula, C. B.; Montanari, C. A.; Oliva, G.; Andricopulo, A. D. Two- and Three-Dimensional Quantitative Structure–Activity Relationships for a Series of Purine Nucleoside Phosphorylase Inhibitors. *Bioorg. Med. Chem.* **2006**, *14*, 516–527.
- (52) Honório, K. M.; Polikarpov, I.; Garratt, R.; Andricopulo, A. D. 3D QSAR Comparative Molecular Field Analysis on Nonsteroidal Farnesoid X Receptor Activators. *J. Mol. Graph. Modell.* **2008**, *25*, 921–927.
- (53) Andrade, C. H.; Salum, L. B.; Castilho, M. S.; Pasqualoto, K. F. M.; Ferreira, E. I.; Andricopulo, A. D. Fragment-Based and Classical Quantitative Structure–Activity Relationships for a Series of Hydrazides as Antituberculosis Agents. *Mol. Divers.* **2008**, *12*, 47–59.
- (54) Salum, L. B.; Polikarpov, I.; Andricopulo, A. D. Quantitative Structure–Activity Relationships for a Series of Selective Estrogen Receptor- β Modulators. *SAR/QSAR Environ. Res.* **2007**, *18*, 711–727.
- (55) Gao, H.; Katzenellenbogen, J. A.; Garg, R.; Hansch, C. Comparative QSAR Analysis of Estrogen Receptor Ligands. *Chem. Rev.* **1999**, *99*, 723–744.
- (56) Demyttenaere-Kovatcheva, A.; Cronin, M. T.; Benfenati, E.; Roncaglioni, A.; Lopiparo, E. Identification of the Structural Requirements of the Receptor-Binding Affinity of Diphenolic Azoles to Estrogen Receptors α and β by Three-Dimensional Quantitative Structure–Activity Relationship and Structure–Activity Relationship Analysis. *J. Med. Chem.* **2005**, *48*, 7628–7636.
- (57) Tong, W.; Perkins, R.; Xing, L.; Welsh, W. J.; Sheehan, D. M. QSAR Models for Binding of Estrogenic Compounds to Estrogen Receptor α and β Subtypes. *Endocrinology* **1997**, *138*, 4022–4025.
- (58) Manas, E. S.; Unwalla, R. J.; Xu, Z. B.; Malamas, M. S.; Miller, C. P.; Harris, H. A.; Hsiao, C.; Akopian, T.; Hum, W. T.; Malakian, K.; Wolfrom, S.; Bapat, A.; Bhat, R. A.; Stahl, M. L.; Somers, W. S.; Alvarez, J. C. Structure-Based Design of Estrogen Receptor- β Selective Ligands. *J. Am. Chem. Soc.* **2004**, *126*, 15106–15119.
- (59) Hsieh, R. W.; Rajan, S. S.; Sharma, S. K.; Guo, Y.; DeSombre, E. R.; Mrksich, M.; Greene, G. L. Identification of Ligands with Bicyclic Scaffolds Provides Insights into Mechanisms of Estrogen Receptor Subtype Selectivity. *J. Biol. Chem.* **2006**, *281*, 17909–17919.
- (60) Goodford, P. J. A Computational Procedure for Determining Energetically Favorable Binding Sites on Biologically Important Macromolecules. *J. Med. Chem.* **1985**, *28*, 849–857.
- (61) Pastor, M.; Cruciani, G. A Novel Strategy for Improving Ligand Selectivity in Receptor-Based Drug Design. *J. Med. Chem.* **1995**, *38*, 4637–4647.
- (62) Filippini, E.; Cecchetti, V.; Tabarrini, O.; Bonelli, D.; Fravolini, A. Chemometric Rationalization of the Structural and Physicochemical Basis for Selective Cyclooxygenase-2 Inhibition: Toward More Specific Ligands. *J. Comput.-Aided Mol. Des.* **2000**, *14*, 277–292.
- (63) Kastenholz, M. A.; Pastor, M.; Cruciani, G.; Haaksma, E. E.; Fox, T. GRID/CPCA: A New Computational Tool To Design Selective Ligands. *J. Med. Chem.* **2000**, *43*, 3033–3044.
- (64) Terp, G. E.; Cruciani, G.; Christensen, I. T.; Jørgensen, F. S. Structural Differences of Matrix Metalloproteinases with Potential Implications for Inhibitor Selectivity Examined by the GRID/CPCA Approach. *J. Med. Chem.* **2002**, *45*, 2675–2684.
- (65) Collini, M. D.; Kaufman, D. H.; Manas, E. S.; Harris, H. A.; Henderson, R. A.; Xu, Z. B.; Unwalla, R. J.; Miller, C. P. 7-Substituted 2-phenyl-benzofurans as ER β Selective Ligands. *Bioorg. Med. Chem. Lett.* **2004**, *14*, 4925–4929.

CI8002182